A Compact Lightweight Aerosol Spectrometer Probe (CLASP)

MARTIN K. HILL, BARBARA J. BROOKS, SARAH J. NORRIS, MICHAEL H. SMITH, AND IAN M. BROOKS

University of Leeds, Leeds, United Kingdom

GERRIT DE LEEUW

TNO, Defence Security and Safety, The Hague, Netherlands, and University of Helsinki, Helsinki, Finland

(Manuscript received 9 August 2007, in final form 26 February 2008)

ABSTRACT

The Compact Lightweight Aerosol Spectrometer Probe (CLASP) is an optical particle spectrometer capable of measuring size-resolved particle concentrations in 16 user-defined size bins spanning diameters in the range $0.24 < D < 18.5$ μm at a rate of 10 Hz. The combination of its compact nature and lightweight and robust build allows for deployment in environments and locations where the use of the larger, heavier, more traditional instrumentation would prove awkward or impossible. The high temporal resolution means it is particularly suited to direct measurements of aerosol fluxes via the eddy covariance technique. CLASP has been through an extended evolutionary development. This has resulted in an instrument whose performance characteristics are well established.

1. Introduction

Sources and sinks of atmospheric aerosol are a key component of the climate system, affecting the global radiation budget both directly, via scattering of incoming solar radiation, and indirectly via their effect on cloud properties. Primary aerosol derived from natural sources include biogenic materials from natural forest fires, pollens, spores, sea salt, and volcanic ash; secondary sources include aerosol arising from the conversion of dimethyl sulfide to sulfates and from the condensation of organic gases.

The magnitude of aerosol sources and sinks remains one of the major areas of uncertainty in climate models. Improving the parameterization of aerosol processes in numerical models requires a better understanding of both the physical and chemical processes that control aerosol formation, their size distributions, chemical reactions with gases, and physical interactions with clouds. Most attempts to characterize source fluxes have relied upon indirect methods; direct measurement of the flux via eddy covariance provides a much more robust estimate, but has been attempted in only a small number of studies (Nilsson et al. 2001; Geever et al. 2005; de Leeuw et al. 2007). Direct eddy covariance has been used more widely to estimate aerosol deposition fluxes over forests (e.g., Gallagher et al. 1997; Buzorius et al. 1998). All previous direct flux estimates, however, have suffered from the limitations of existing instrumentation. Optical particle spectrometers capable of providing detailed size spectra typically have a temporal resolution no better than 1 Hz, and thus cannot resolve all the turbulent fluctuations in particle concentration; they also tend to be bulky and require a long sample line between the instrument and the sampling location—this incurs loss of particles to the wall of the sample line, introduces a lag time between aerosol and sonic turbulence wind measurements, and may further reduce the frequency response due to mixing within the sample line. A temporal resolution of order 10 Hz—sufficient to resolve the relevant scales—can be achieved with condensation particle counters, but they provide no direct information on particle size. A more extensive discussion of the instrumentation available for the measurement of aerosol size distributions and the relative merits and disadvantages of the physical properties exploited can be found in Reid et al. (2003, 2006). Traditional aerosol instruments are also typically ill suited for applications such as balloonborne measurements or for use in confined or highly exposed locations because of their size, weight, power require-

Corresponding author address: Dr. Sarah J. Norris, School of Earth and Environment, University of Leeds, Leeds, LS2 9JT, United Kingdom.
E-mail: s.norris@see.leeds.ac.uk

DOI: 10.1175/2008JTECHA1051.1

ments, and cost. To meet the requirements for a small, compact, lightweight, fast response, and relatively inexpensive particle spectrometer, the University of Leeds has developed the Compact Lightweight Aerosol Spectrometer Probe (CLASP).

2. The CLASP instrument

a. The scatter cell

CLASP is built around a commercially available scatter cell, designed and manufactured by Pacific Scientific Instruments, Oregon, and used in their range of handheld, portable, and bench-top particle counters. The same scatter cell was used by Clarke et al. (2002) in the development of a miniature optical particle counter (OPC). Clarke et al. obtained their scatter cell by removing it from a MetOne model 237A particle counter and refer to the scatter cell by this model number. For CLASP the scatter cells were sourced directly from the manufacturer and will be referred to simply as a MetOne scatter cell for clarity rather than by a particular MetOne product model number.

The chamber of the scatter cell is cylindrical, approximately 25 mm in depth and 19 mm in diameter with a concave, gold-plated mirror fitted into one end; this can be removed to access the cell. A schematic representation of the scatter cell is shown in Fig. 1. The aerosol sample stream enters the scatter chamber through a 2.4-mm-diameter inlet, extending 7.5 mm into the chamber and orthogonal to the laser path. The sample flow exits through a 2.4-mm-diameter opening in the chamber wall directly opposite the inlet.

The laser source is a low-output power (15 mW), 780-nm wavelength laser diode. A built-in photodiode is used in an optoelectronic feedback loop to regulate the diode current and keep beam power constant. This feedback loop is incorporated into the laser diode drive circuitry supplied by the manufacturer and mounted on the body of the scatter cell. As the diode ages the current required to maintain the same beam power increases. The maximum operational voltage is approximately 2.4 V and is reached shortly before the laser fails. The laser diode operational voltage, a measure of this regulated drive current is available as an output from the drive circuit and used by CLASP to monitor the "health" of the diode, allowing replacement prior to failure. Laser diodes of this type operate in a single spatial mode for both axes and the beam that emerges is wedge shaped, highly divergent ($10° \times 30°$) and linearly polarized: typical beam dimensions being 3×1 mm. The beam enters the chamber through a cylindrical lens with a focal length of 20 mm (Clarke et al. 2002). The beam exits the chamber through a 6-mm-diameter duct into a dump spot. Clarke et al. (2002) characterized the optical geometry of the cell; the focusing lens brings the laser to a wedge-shaped sheet spanning the entire width of the sample flow, thus all particles entering the system pass through the beam. At the point at which it first intercepts the sample flow the beam is approximately 0.1 mm thick; at the focal point, approximately 1 mm beyond the center of the aerosol stream, the width is presumed diffraction limited, about 1–1.5 μm thick. We note that Clarke et al. narrowed the sample inlet tube to 1.6 mm in their mini-OPC; no such modification has been made in CLASP with the result that the maximum beamwidth will be about 2% greater than for Clarke et al. The maximum transit time for a particle through the laser is approximately 9 μs. The scattering volume is approximately 0.21×10^{-9} m^3; thus at a particle concentration of approximately 5000 mL^{-1} an average of more than 1 particle would be in the scatter volume at any given time.

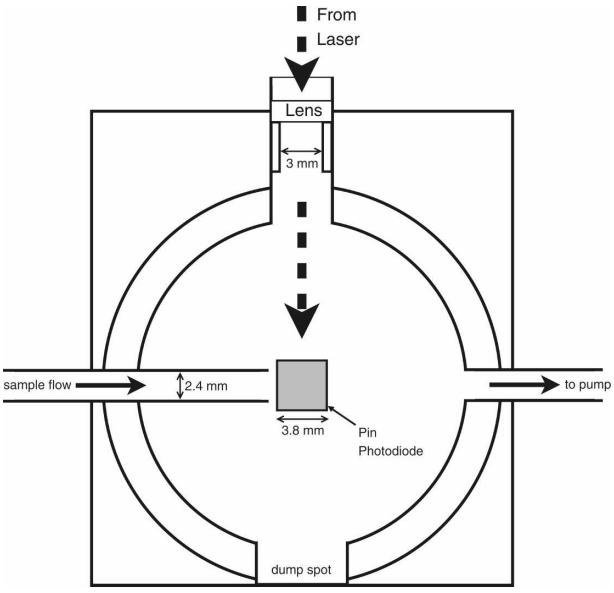

FIG. 1. A schematic illustration of the of the MetOne scatter cell (approximately to scale).

A silicone PIN-type 3.8 mm $\times$ 3.8 mm photodiode with a sensitivity of 0.6 A W^{-1} is mounted below the scatter volume, diametrically opposite the concave mirror. The optical configuration is illustrated in Fig. 2. The intersection of the particle stream and the laser is situated between the center of curvature c and the focal point f of the mirror. The mirror subtends an angle of approximately 100° with the scatter volume along both the laser and particle trajectory axes, providing an effective collection angle of approximately 90°; while the photodiode subtends a collection angle of approxi-

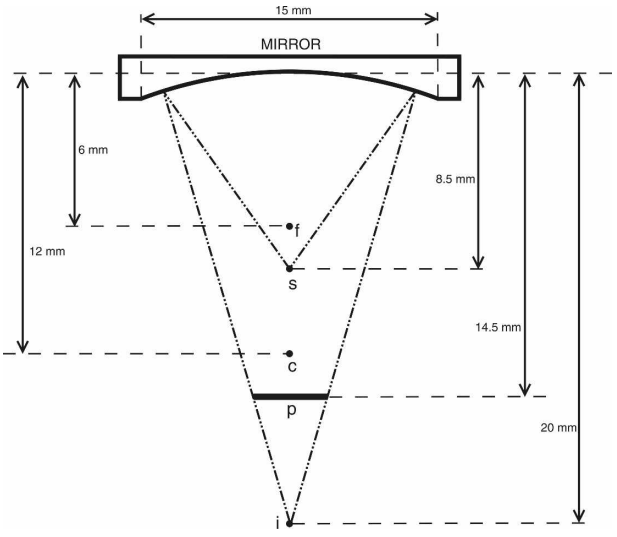

FIG. 2. A schematic illustration of the optical paths within the MetOne scatter cell. The marked points denote f the focus of the mirror, s the center of the sample volume, c the center of curvature of the mirror, i the image of the particle, and p the photodiode.

mately 35° with the scatter volume. The initial amplification of the photodiode output is performed by the manufacturer's proprietary electronics; this amplified signal is then fed through a purpose-built pulse height analyzer, described in section 3.

b. Modeling of scattering properties

The commercial instruments from which the MetOne scatter cell is taken do not provide a fully size-resolved aerosol spectrum. To determine the response to particle size to be expected from the scatter cell, and confirm its suitability for providing detailed size spectra, it was modeled using Mie theory (van de Hulst 1982) for particles in the size range 0.1 μm $< R <$ 10 μm and of six different compositions: water, sea salt, soot, water soluble sulfate, dust, and polystyrene calibration beads. The composition of a particle affects the complex refractive index and thus the scattering characteristics and resultant intensity pattern. Table 1 shows the complex refractive indices used in the model. The validity of the model was first tested by applying it to the optical configuration of a Particle Measurement Incorporated (PMI) Forward Scattering Aerosol Spectrometer Probe (FSSP) and comparing the scattering cross section with those derived for the same instrument by Shettle and Fenn (1979). The FSSP light source is a 633-nm helium–neon laser with a collection angle of 3° to 13°. Figure 3a shows the modeled variation of scattering cross section per particle for the FSSP and is in exact agreement with

TABLE 1. Refractive indices of aerosol components for light sources of wavelengths 633 and 780 nm (Shettle and Fenn 1979; and Duke Scientific).

	780 nm	633 nm
Water	$1.329 - 3.29e^{-7}i$	$1.332 - 1.46e^{-8}i$
Sea salt	$1.48 - 3.e^{-6}i$	$1.49 - 2e^{-8}i$
Soot	$1.75 - 0.43i$	$1.75 - 0.43i$
Dust	$1.52 - 8e^{-3}i$	$1.53 - 8e^{-3}i$
Water soluble	$1.52 - 1.2e^{-2}i$	$1.53 - 6e^{-3}i$
PSL (Duke Scientific)	1.59	1.59

the findings of Shettle and Fenn (1979). The results from the FSSP test case indicate that the model is effectively accounting for the optical arrangement of the instrument and the variation of refractive index. Figure 3b shows the scattering cross section per particle for the same size range and compositions for the MetOne scatter cell.

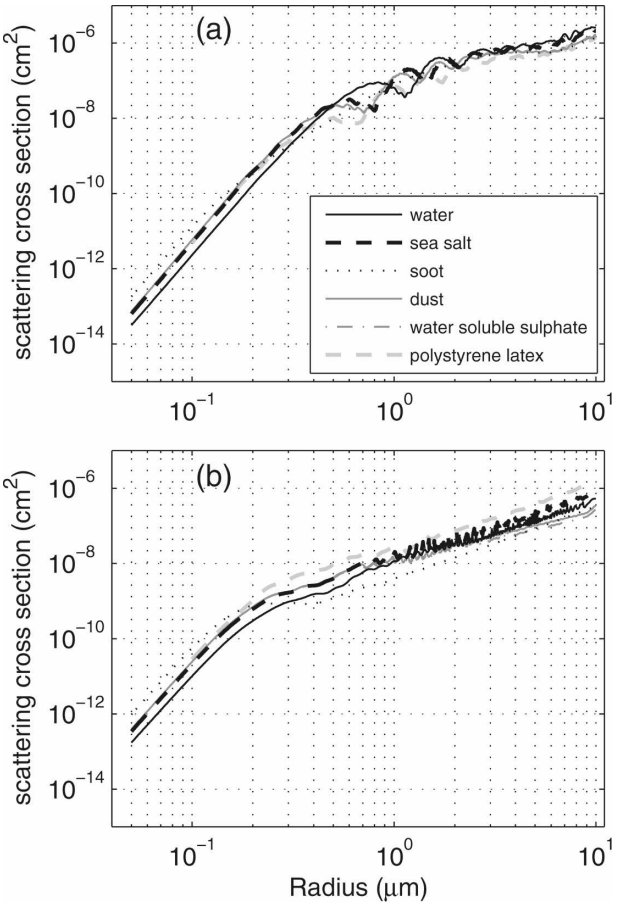

FIG. 3. Scattering cross section per particle for different particle compositions for (a) the PMI FSSP, laser wavelength 635 nm; and (b) MetOne scatter cell, laser wavelength 780 nm. Complex refractive indices for each particle type are shown in Table 1.

Consider the response of both the FSSP and MetOne in the 1-μm region. The variations in scattering response are much more pronounced in the case of the FSSP than for the MetOne. This results from differences in the instrument optics. The FSSP samples a narrow cone of forward-scattered light within the angles of 3° to 13°, whereas the MetOne collects side-scattered light. Since the side lobes in the Mie scattering patterns vary with particle size to a much lesser extent than the forward lobe (Brooks 2002), the response curves for the MetOne are nearly monotonic with particle size, apart from the results for soot. Periodicities in the response curves for the FSSP for particles around 1 μm give rise to a multivalued response in this region, which remains a cause of concern for many scientists using this instrument. A further noticeable point is the markedly different response of each probe to soot particles compared with particles of other compositions, as a consequence of the highly absorbing nature of soot (and hence a larger imaginary component of its refractive index) at 633 and 780 nm. The effect on the FSSP is to dampen out variations in the scattering component, thereby smoothing its response curve. The MetOne displays a reduced and flatter curve than for the other compositions, especially for particle radii from 0.2 to 5 μm, because of greater absorption of the incident beam by soot than for the other particle compositions. The Mie scattering model results suggest that the MetOne scatter cell should be well suited for use in a fully size-resolving aerosol spectrometer.

3. CLASP electronics

During the development of CLASP, the signal processing electronics has progressed through three versions of the pulse height analyzer (PHA) and associated electronics, each of which has been tested during field deployments and has built upon the experience gained with the earlier versions. The third and most versatile variant is now in active use and is discussed in detail below.

The current version of CLASP was designed for long-term deployment in inaccessible locations and for making eddy covariance measurements of aerosol fluxes. The complete system is built on one printed circuit board and includes a sample air pump, sample flow-rate monitoring and control, a 1024-channel pulse height analyzer, sample head monitoring and control, sample cell mirror heating, temperature monitoring and control, a full-duplex RS485 communications link, and all necessary power supplies to allow the unit to operate from an external 24-V supply. The board does not store long-term data locally; acquired data is transmitted via the serial interface to a separate logging computer. The system is built around an Atmel Microcontroller (Atmel MEGA32) which has internal static memory, flash program memory, and many peripherals such as a serial data controller used here for RS485 communications. The device also contains a section of electrically erasable programmable read-only memory (EEPROM) nonvolatile memory that is used for storing operational configuration parameters. A block diagram of the system is shown in Fig. 4.

a. Pulse height analyzer (PHA)

The PHA uses a combination of two triggers to cause a medium-fast 10-bit analog-to-digital convertor (ADC; National Semiconductors ADC1016) to convert at the peak of the pulse. The input pulse is compared to a threshold, as set by the output of the 12-bit output of the digital-to-analog convertor (DAC); if its amplitude exceeds the threshold, the output of voltage comparator 1 (CMP1) goes high, causing the data (D) input of the first "D"-type flip-flop to be set to logic "1." In D-type flip-flop (FF), the Q output follows the D input when the CLK signal is high, and latches this state when the clock (CLK) is low. The pulse signal also goes to a second comparator, via a 10-nF capacitor, loaded by a 1-kΩ resistor. The combination of these two components causes the first derivative of the pulse waveform to be applied to the negative input of CMP2, the positive input being at ground potential. On the rising edge of the pulse, the positive slope causes CMP2 to be held with its output low, as the negative input is at a higher potential than the positive input. At the peak of the waveform, the slope makes the transition from positive to negative, and hence the input to CMP2 rapidly goes through zero to a negative potential. The output of CMP2 goes high when the through-zero transition occurs, causing the data on the D input of FF1 to be transferred to its Q output. The rising edge of the Q output of FF1 causes FF2 to change state, with Q going low. This transition causes the ADC to start a conversion, the first phase of which is for the internal track-and-hold amplifier to go into "hold" mode. This occurs within 1 μs of the peak of the waveform. Approximately 2 μs after the trigger, the ADC completes its conversion and signals this state to the microcontroller. Inside the microcontroller, this signal causes an interrupt service routine to be invoked, which reads the 10-bit result, processes the data then toggles the PHA reset line, causing both FF1 and FF2 to reset, readying the PHA for a new event. The total cycle time for the PHA is approximately 5 μs. The 1-MΩ–1-kΩ resistor combination on the positive inputs of the comparators provides a 5-mV hysteresis for stability. With this PHA

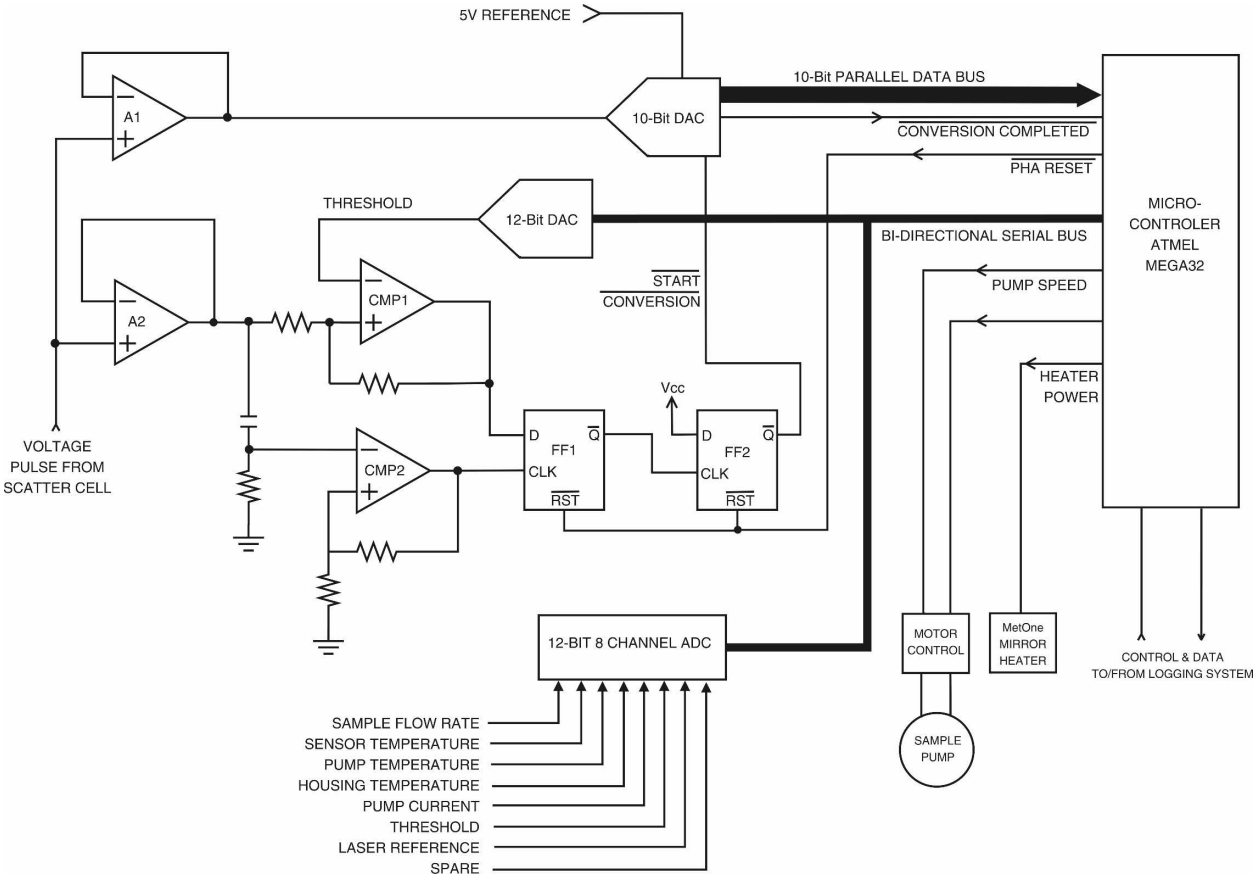

FIG. 4. Outline schematic of CLASP pulse height analyzer electronics.

cycle time the electronics are capable of dealing with a maximum of 200 000 cps. The sample flow rate is 50 mL s^{-1}, resulting in a maximum measurable concentration of 4000 mL^{-1}, about 80% of the concentration at which coincidence errors become ubiquitous; the maximum particle concentration that can be measured is thus determined primarily by the signal processing electronics rather than the optical sample volume. The velocity of the sample stream as it passes through the sample volume is approximately 11.1 m s^{-1} and the maximum transit time through the laser path approximately 9 μs. Total particle concentrations should be increased slightly to allow for the dead time of the instrument following detection of a particle; the fractional undercount increases linearly with the particle concentration 0.25% at 10 mL^{-1}, 2.5% at 100 mL^{-1}.

The arrangement of comparators and flip-flops used here has proved to be greatly immune to false triggers: noise on the "zero crossing" comparator has no effect unless the signal pulse is greater than the threshold setting (in which case it is likely to be a real event); noise on the threshold comparator is only relevant if synchronous with a noise event on the zero crossing comparator. The arrangement has one further benefit: the signal from the sensing head has, when the aerosol concentration is high, frequent "multipeaked" pulses caused by the pulse from one aerosol particle overlapping with those from other particles. In these events, the waveform does not drop back to the baseline before the next peak. The arrangement above allows these additional peaks to be analyzed, even though the signal does not drop back below the threshold. Laboratory tests using a calibrated pulse generator show that the reported pulse height is within 5 mV of the true value.

b. Firmware

A 10-bit ADC was adopted because its resolution, approximately 5 mV per bit, allows accurate setting of the threshold for the pulse magnitude comparator, thus permitting the system to be able to see particle events only marginally above the noise floor. Storing data from 1024 channels would, however, be profligate. Instead, the 10-bit information is used as a vector into a 1024-element array. The array is preset, on system initialization, so that each element contains the channel number of the output histogram to which a particular

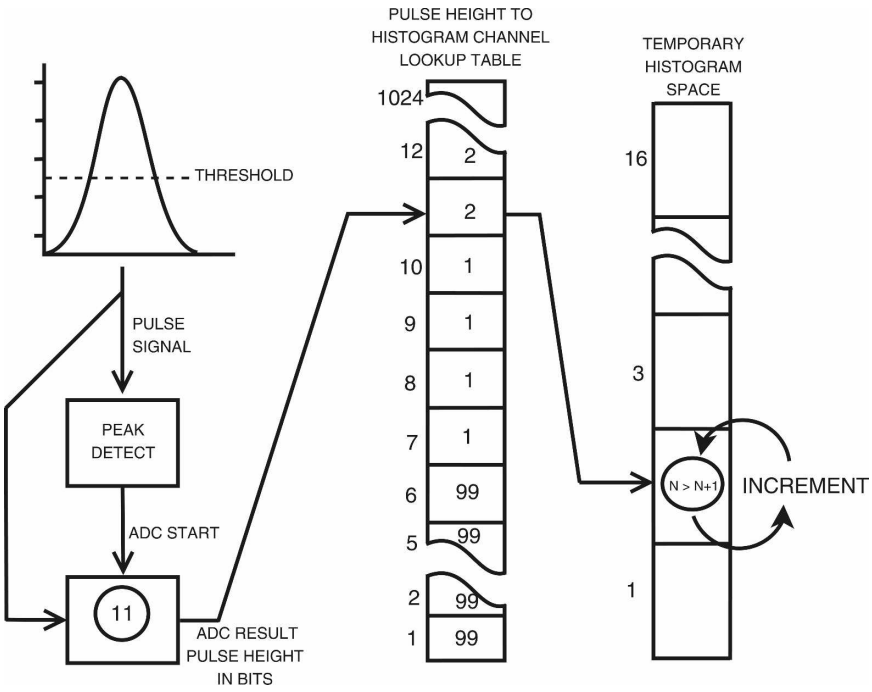

FIG. 5. Logic flow for the PHA lookup processor.

voltage is assigned. Table entries with the channel number 99 are for voltages outside the output histogram space, either undersize or oversize, and are dealt with separately. Table entries in the "normal" range are used as new vectors to a temporary histogram space; the referenced element in the histogram is incremented. This lookup process is shown diagrammatically in Fig. 5. The number of channels in the output histogram can be set to any reasonable value depending on the expected number concentration, required precision and required output frequency. The current version of the firmware constrains the number of channels to 16. The histogram formation rate is also variable over a wide range, but is set at 10 Hz in the current firmware.

The data acquisition cycle is initiated by the host computer sending a "Go" command. The temporary histogram space is cleared and the PHA enabled. Every 100 ms the temporary histogram is copied to a circular buffer and the temporary space is cleared. The data can be sent automatically to the host computer at fixed intervals, or can be accumulated in the circular buffer until a request is received from the host. The circular buffer also contains an additional parameter with each histogram. The content of this parameter cycles with each sample through a list of "housekeeping" data such as a count of undersize–oversize events, the sample flow rate, pump current, laser voltage, and the temperatures of mirror, pump, and enclosure.

To facilitate generation of the voltage-to-channel lookup table, the unit can be configured so that the 10-bit ADC conversion result is sent directly to the host computer in real time, bypassing the lookup routine. This allows for a 1024-channel histogram to be built in an external computer, synchronously with a histogram from a "standard" spectrometer, such as the PMI Passive Cavity Aerosol Spectrometer Probe (PCASP). With data from both instruments when sampling ambient aerosol or calibration particles, an accurate transfer function of the 1024 input channels to 16 output channels can be created.

Initialization routines are included to automatically fill the 1024-element lookup table from the histogram channel boundaries, which are initially sent by the host computer. Once loaded into the unit, these boundaries can also be saved in the nonvolatile EEPROM for automatic retrieval when the system is powered up. Flow-rate setting, PHA threshold, and other basic operational parameters are also stored in EEPROM. The firmware also includes the necessary routines for maintaining constant sample flow, maintaining the mirror of the sample cell above ambient temperature, and monitoring for fault conditions such as excessive pump temperature or sample cell laser failure.

The physical size of the CLASP unit has been kept as small as possible in order to allow the entire system to be housed in a compact enclosure. The physical footprint of the current CLASP model is 25 cm $\times$ 8 cm $\times$ 6 cm with a weight of approximately 500 g. This com-

TABLE 2. Size, tolerance, and composition of the Duke Scientific standard particles used in the calibration of CLASP.

Diameter (μm)	Tolerance (μm)	Composition
15.5	1.1	Borosilicate glass
14.5	1	Borosilicate glass
8.2	0.8	Borosilicate glass
7.9	0.8	Borosilicate glass
5.1	0.5	Borosilicate glass
2.5	0.5	Borosilicate glass
2.1	0.5	Borosilicate glass
1.1	0.005	Borosilicate glass
0.794	0.004	Borosilicate glass
0.701	0.006	PSL water suspension
0.491	0.004	PSL water suspension
0.35	0.007	PSL water suspension
0.3	0.006	PSL water suspension

pact size allows CLASP to be sited close to a sonic anemometer in order to make direct eddy correlation estimates of aerosol fluxes without introducing a significant source of flow distortion, and minimizing particle losses within the inlet tube. The use of CLASP in the field is discussed briefly in section 5.

4. Calibration

The aim of the calibration is to determine the mapping of the 1024 PHA output channels to physical particle size, and to verify the counting efficiency.

a. Lower threshold determination

The minimum signal threshold represents the thermal noise level of the electronics, including the PIN photodiode, and is the minimum meaningful value for the lower boundary of the first of the 16 user-definable channel boundaries. It is determined by placing an absolute High Efficiency Particulate Air (HEPA) filter on the inlet and increasing the lowest channel boundary until no counts are recorded. For the CLASP unit used here as an example this lower threshold was found to be PHA channel 13 (65 mV).

b. Calibration with particle standards

The calibration was carried out with particle standards supplied and assayed by Duke Scientific Corporation. They comprised water suspension of polystyrene latex (PSL) particles for diameters below 0.7 μm, and dry borosilicate glass spheres for large particles; the sizes, tolerances, and compositions of particles used are given in Table 2. The PSL solutions were diluted 10:1 with 20 MΩ water before atomization. An absolute air source was used to ensure no contamination of the calibration aerosol occurred. Drying of the aerosol stream

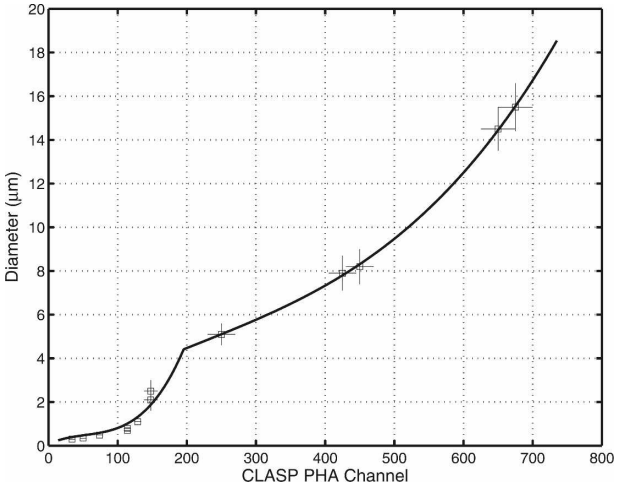

FIG. 6. Calibration curve obtained using a mixture of Duke Scientific PLS and glass calibration particles. Error bars represent the stated tolerances of the particle standards and the width of the PHA channel distributions. The fitted curve is restricted to the PHA channels within the determined threshold limits.

was achieved by mixing with heated, dry absolute air. The calibration particles were sampled by a PCASP as well as CLASP to verify that they fell into the expected PCASP channels. The borosilicate spheres were introduced to both instruments by lofting particles from a spatula within the airstream into the instrument inlets. The peaks of the resulting distributions define the PHA channel number corresponding to each particle size; the width of the distribution provides a measure of the uncertainty in the sizing. Tests with a particle standard of diameter 19.9 $\pm$ 1.4 μm (not shown) failed to properly resolve the peak, although some particles were detected. This suggests that the detection limit lies just under 19 μm, at the lower end of the tolerance range for this set of standard particles. The upper detection threshold was determined by using 20-μm calibration particles and adjusting the lower limit of the upper size bin until no particle counts were detected. The upper threshold was found to be PHA channel 735 (3.675 V).

Figure 6 shows the calibration curve for one particular CLASP unit. It can be seen that it is necessary to fit two separate curves over different size ranges. This is a primarily a result of the nonlinear signal amplification; transitions between Rayleigh, Mie, and geometric scattering may also contribute to the nonlinearity. The minimum particle diameter resolved is 0.24 μm at the lower noise threshold; the maximum is 18.5 μm.

c. Intercomparison with PCASP

With the size calibration in place an intercomparison was performed with a PMI PCASP in order to verify the counting statistics. The PCASP has a size range of

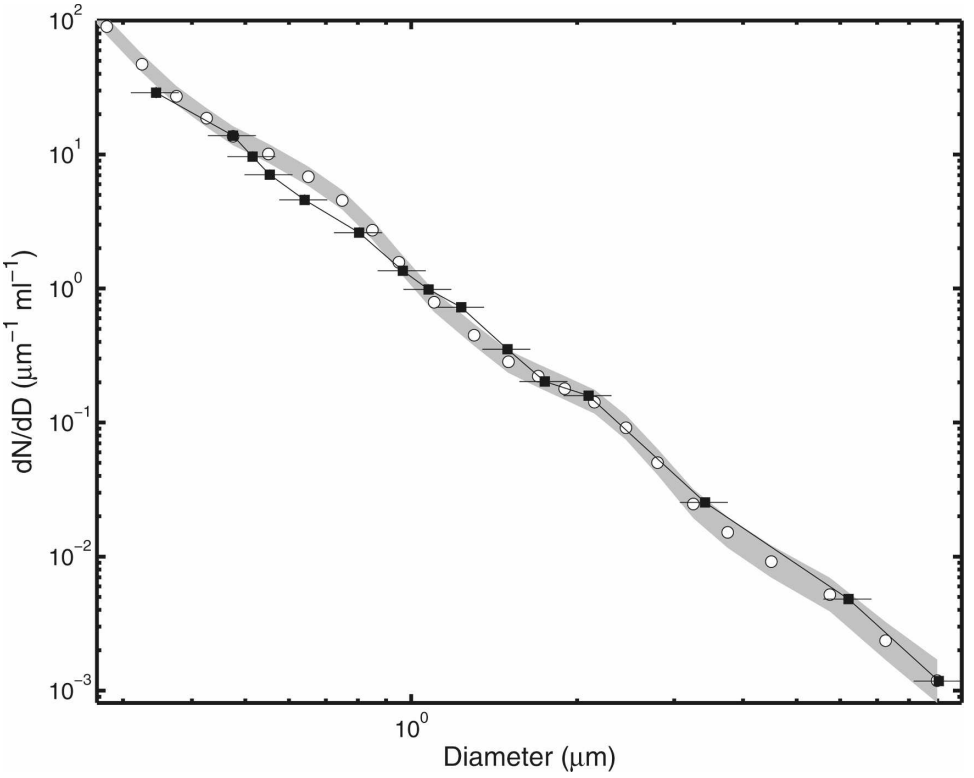

FIG. 7. Intercomparison of CLASP (■) and PCASP (○) derived size spectra. The shaded area indicates the uncertainty in the PCASP concentrations—a combination of the standard error in the mean counts in each channel, and an estimated uncertainty in the channel width of 10%. The horizontal error bars on the CLASP concentrations show the uncertainty in particle size. The high sample volume of CLASP provides much better counting statistics than the PCASP, and the vertical error bars are almost all smaller than the plotted symbol.

$0.1\ \mu m < D < 10\ \mu m$; CLASP channel boundaries were set to constrain the upper and lower measurement limits within the range 0.3 and 10 μm, corresponding to the PCASP channels 8–31. Sampling from laboratory air for a period of approximately 1 h the total number concentrations within the selected size range were $9.69 \pm 0.04\ mL^{-1}$ for the PCASP and $9.36 \pm 0.02\ mL^{-1}$ for CLASP. Figure 7 shows a full spectral comparison between the two instruments. The degree of conformity between both the spectral and total number measurements indicates that CLASP is successfully sampling all the particles in the sample stream and that the size calibration is acceptable.

5. Research applications for CLASP

CLASP has undergone extensive field use in multiple campaigns during its development. The initial prototype was used on a tethered balloon to obtain aerosol profiles at a coastal site during the North Atlantic Marine Boundary Layer Experiment (NAMBLEX) field campaign (Heard et al. 2006). A second version was tested during the Waves Air–Sea interactions, Fluxes, Aerosols and Bubbles (WASFAB) field campaign in Duck, North Carolina, (de Leeuw et al. 2007). This version provided only 8 size channels but achieved the first size-resolved estimates of sea spray aerosol fluxes via eddy correlation (Norris et al. 2008). Several individual units of the current version of CLASP were deployed during the Sea Spray, Gas Flux and Whitecaps (SEASAW) project (Brooks et al. 2007)—a study of sea spray aerosol and air–sea gas fluxes under high wind conditions. Three CLASP units were mounted within weatherproof enclosures (Fig. 8) alongside a sonic anemometer, LI-COR LI-7500 open-path CO_2–H_2O gas analyzer and a motion package on the foremast of the RRS *Discovery* at 21 m above the surface (Fig. 9) to make eddy correlation flux measurements (Norris et al. 2007a). An example of the sea spray source function derived from the flux measurements is shown in Fig. 10 alongside other source functions from the recent literature (see Norris et al. 2008 for refer-

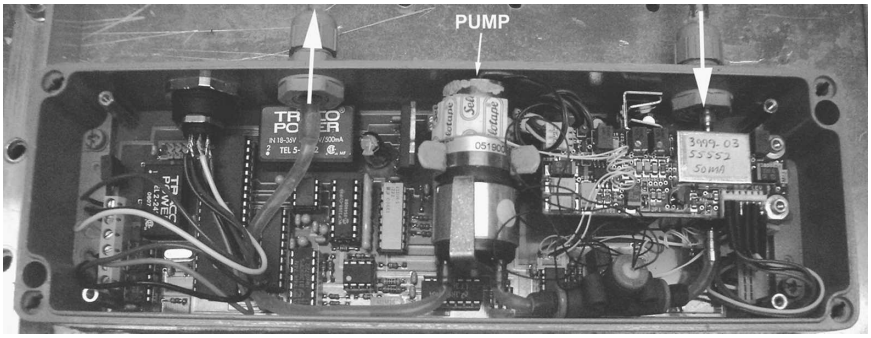

FIG. 8. The current version of CLASP within its weatherproof enclosure (opened). Arrows indicate flow into the scatter cell at top right and out of the instrument at top left. The flow passes a mass flow sensor before being drawn through the pump. The enclosure is 25 cm long.

ences). Two further units were mounted on a tethered buoy to measure the particle spectra within 1 m of the surface (Fig. 11) in order to assess particle production associated with individual whitecaps (Norris et al. 2007b). A motion pack on the buoy allows the 10-Hz aerosol data to be related to position on the waves. More recently a CLASP unit has been deployed on the ASIS buoy (Graber et al. 2000)—an autonomous spar buoy for air–sea interaction studies. Such near-surface measurements at sea would not be possible with traditional aerosol instrumentation, not least because they carry a significant risk from waves inundating the instrument. CLASP units have been submerged on two occasions during about a dozen deployments. On both occasions the pumps have suffered complete failure. The sample flow path through the instrument is sealed, however, and no water escaped into the electronics enclosure. After careful cleaning and drying of the scatter cell, and replacement of the pump, the instruments have continued to operate normally. This robust nature, coupled with the relatively low cost compared to most traditional aerosol instruments, makes such risky deployments viable, enabling the collection of unique near-ocean-surface measurements.

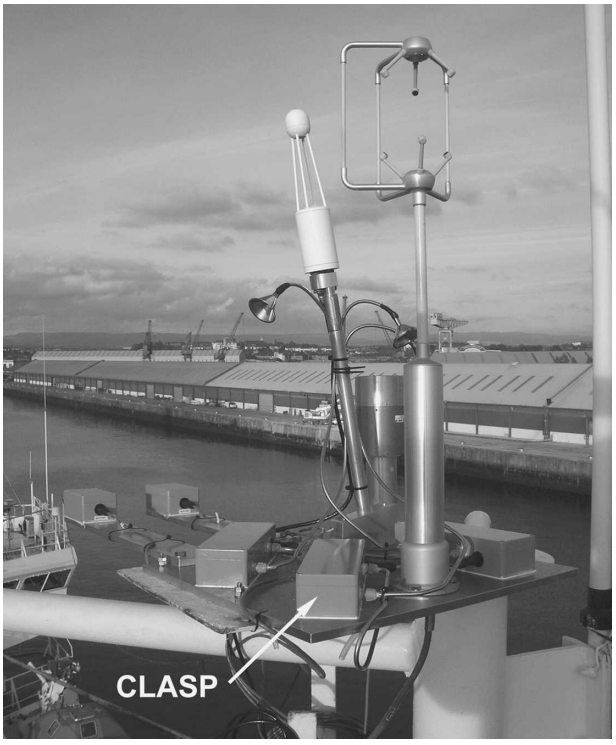

FIG. 9. The CLASP units mounted alongside a sonic anemometer and a LICOR LI-7500 gas analyzer at the top of the foremast of the RRS *Discovery* for the United Kingdom–Surface Ocean–Lower Atmosphere Study (UK–SOLAS) SEASAW cruise.

6. Summary

CLASP is a compact lightweight optical particle counter with a fast sample rate and high sample volume

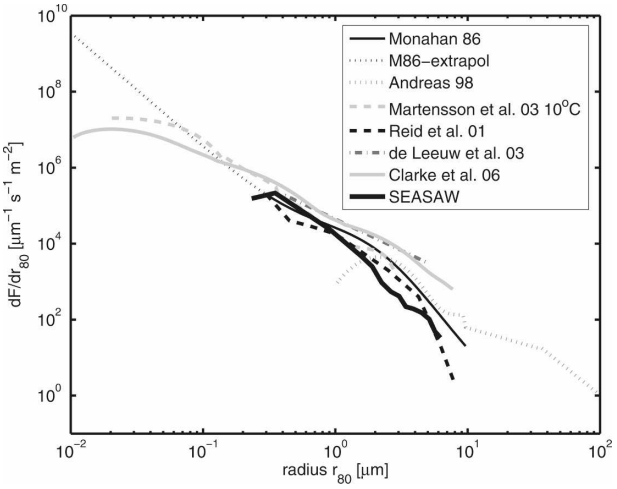

FIG. 10. Example sea spray source functions for a wind speed of 10 m s^{-1}; all functions are normalized for aerosol equilibrium sizes at a relative humidity of 80%.

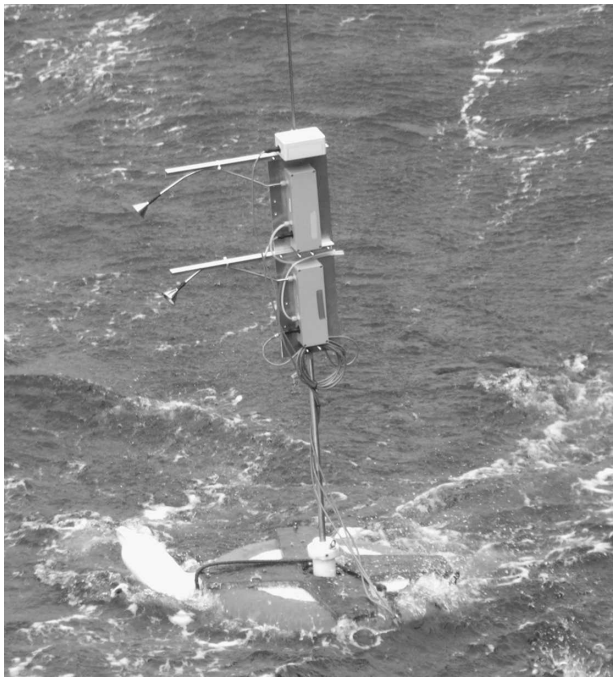

FIG. 11. Two CLASP units mounted on a small tethered buoy making near-surface aerosol measurements in the North Atlantic during the SEASAW cruise.

flow allowing high temporal resolution (10 Hz) measurements of particle size distributions to be obtained. Particles are sized into 16 user-configurable size bins spanning diameters in the range $0.24 < D < 18.5$ μm. The current version of CLASP, housed in a weatherproof enclosure measures approximately $25 \times 8 \times 6$ cm and weighs approximately 0.5 kg, allowing collocation with a sonic anemometer for measurement of aerosol fluxes by eddy covariance or deployment in locations where use of traditional instrumentation would not be feasible—such as on buoys. It is capable of operating for periods of several weeks with no user intervention, and has proved extremely robust, allowing deployment in harsh environments where the risk of damage to the instrument is a significant possibility. CLASP continues to undergo development for use in a wide variety of applications, including a more compact, lower-power version for balloonborne measurements.

Acknowledgments. During the development of CLASP, which was protracted by the serious illness of its principal designer, a number of agencies provided financial and other support. The UK Natural Environment Research Council funded the development of the initial prototype through its COSMAS program (NER/T/S/200/01184), its field deployment was funded by NERC's NAMBLEX project (NER/A/S/2000/01313). The buoy prototype was tested during a field trial on the German Baltic coast funded by Defence Science and Technology Laboratories contract RD023-023-01771. Development of the current version of CLASP was funded by NERC as part of the SEASAW project (NE/C001842/1). The U.S. Office of Naval Research funded development of the Mk 2 instrument (N00014-03-1-0916) and the participation of both Leeds and TNO in the WASFAB project (N00014-96-1-0581). The authors are grateful for the logistical and operation support provided by the Field Research Facility of the U.S. Army Corp of Engineers: Engineering Research and Development Center. Finally, during her involvement in this project, Dr Sarah Norris was in receipt of a postgraduate studentship from TNO, The Hague, Netherlands; this work forms part of her Ph.D. thesis.

REFERENCES

Brooks, B. J., 2002: COSMAS report. NERC Contract Rep. NER/T/S/2000/01184, University of Leeds, 13 pp.

Brooks, I. M., and Coauthors, 2007: An overview of the Sea Spray, Gas Flux, and Whitecaps (SEASAW) Field Study. Preprints, *15th Conf. on Air–Sea Interaction,* Portland, OR, Amer. Meteor Soc., P12.3. [Available online at http://ams.confex.com/ams/pdfpapers/124982.pdf.]

Buzorius, G., U. Rannk, J. M. Makela, T. Vesala, and M. Kulmala, 1998: Vertical aerosol particle fluxes measured by eddy covariance technique using condensational particle counter. *J. Aerosol Sci.,* **29,** 157–171.

Clarke, A. D., N. C. Ahlquist, S. Howell, and K. Moore, 2002: A miniature optical particle counter for in situ aircraft aerosol research. *J. Atmos. Oceanic Technol.,* **19,** 1557–1566.

de Leeuw, G., M. M. Moerman, C. J. Zappa, W. R. McGillis, S. J. Norris, and M. H. Smith, 2007: Eddy correlation measurements of sea spray aerosol fluxes. *Transport at the Air Sea Interface,* C. S. Garbe, R. A. Handler, and B. Jähne, Eds., Springer-Verlag, 297–311.

Gallagher, M. W., K. M. Beswick, J. Duyzer, H. Westrate, T. W. Choularton, and P. Hummelshoj, 1997: Measurements of aerosol fluxes to Speulder Forest using a micrometeorological technique. *Atmos. Environ.,* **31,** 359–373.

Geever, M., C. D. O'Dowd, S. van Ekeren, R. Flanagan, E. D. Nilsson, G. de Leeuw, and Ü. Rannik, 2005: Submicron sea spray fluxes. *Geophys. Res. Lett.,* **32,** L15810, doi:10.1029/2005GL023081.

Graber, H. C., E. A. Terray, M. A. Donelan, W. M. Drennan, J. C. van Leer, and D. B. Peters, 2000: ASIS—A new air–sea interaction spar buoy: Design and performance at sea. *J. Atmos. Oceanic Technol.,* **17,** 708–720.

Heard, D. E., and Coauthors, 2006: The North Atlantic Marine Boundary Layer Experiment (NAMBLEX). Overview of the campaign held at Mace Head, Ireland, in summer 2002. *Atmos. Chem. Phys.,* **6,** 2241–2272.

Nilsson, E. D., Ü. Rannik, E. Swietlicki, C. Leck, P. P. Aalto, J. Zhou, and M. Norman, 2001: Turbulent aerosol fluxes over the Arctic Ocean 2. Wind driven sources from the sea. *J. Geophys. Res.,* **106,** 32 139–32 154.

Norris, S. J., I. M. Brooks, M. K. Hill, B. J. Brooks, M. H. Smith, and J. J. N. Lingard, 2007a: Eddy correlation measurements

of sea-spray aerosol fluxes during SEASAW. Preprints, *15th Conf. on Air–Sea Interaction,* Portland, OR, Amer. Meteor. Soc., P12.4. [Available online at http://ams.confex.com/ams/pdfpapers/124985.pdf.]

——, ——, M. H. Smith, M. K. Hill, B. J. Brooks, and G. de Leeuw, 2007b: In-situ measurements of aerosol production from individual whitecaps during SEASAW. Preprints, *15th Conf. on Air–Sea Interaction,* Portland, OR, Amer. Meteor. Soc., P1.2. [Available online at http://ams.confex.com/ams/pdfpapers/124984.pdf.]

——, ——, G. de Leeuw, M. H. Smith, M. Moerman, and J. J. N. Lingard, 2008: Eddy covariance measurements of sea spray particles over the Atlantic Ocean. *Atmos. Chem. Phys.,* **8,** 555–563.

Reid, J. S., and Coauthors, 2003: Comparison of size and morphological measurements of coarse mode dust particles from Africa. *J. Geophys. Res.,* **108,** 8593, doi:10.1029/2002JD002485.

——, and Coauthors, 2006: Reconciliation of coarse mode sea-salt aerosol particle size measurements and parameterizations at a subtropical ocean receptor site. *J. Geophys. Res.,* **111,** D02202, doi:10.1029/2005JD006200.

Shettle, E. P., and R. W. Fenn, 1979: Models for the aerosols of the lower atmosphere and the effect of the humidity variations on their optical properties. Air Force Geophysics Laboratory Rep. AFGL-TR-79-0214, Hanscom Air Force Base, Bedford, MA, 94 pp.

van de Hulst, H. C., 1982: *Light Scattering by Small Particles*. Dover, 470 pp.